



TITLE:

Specific gene expression in unmyelinated dorsal root ganglion neurons in nonhuman primates by intra-nerve injection of AAV 6 vector

AUTHOR(S):

Kudo, Moeko; Wupuer, Sidikejiang; Fujiwara, Maki; Saito, Yuko; Kubota, Shinji; Inoue, Ken-ichi; Takada, Masahiko; Seki, Kazuhiko

CITATION:

Kudo, Moeko ...[et al]. Specific gene expression in unmyelinated dorsal root ganglion neurons in nonhuman primates by intra-nerve injection of AAV 6 vector. *Molecular Therapy : Methods & Clinical Development* 2021, 23: 11-22

ISSUE DATE:

2021-12

URL:

<http://hdl.handle.net/2433/265083>

RIGHT:

© 2021 The Author(s).; This is an open access article under the Creative Commons Attribution-NonCommercial-NoDerivatives 4.0 International license.



Specific gene expression in unmyelinated dorsal root ganglion neurons in nonhuman primates by intra-nerve injection of AAV 6 vector

Moeko Kudo,¹ Sidikejiang Wupuer,¹ Maki Fujiwara,² Yuko Saito,³ Shinji Kubota,¹ Ken-ichi Inoue,² Masahiko Takada,² and Kazuhiko Seki¹

¹Department of Neurophysiology, National Institute of Neuroscience, National Center of Neurology and Psychiatry, Kodaira, Tokyo, Japan; ²Systems Neuroscience Section, Department of Neuroscience, Primate Research Institute, Kyoto University, Inuyama, Aichi, Japan; ³Department of Neuropathology, Tokyo Metropolitan Institute of Gerontology, Itabashi, Tokyo, Japan

Adeno-associated virus 6 (AAV6) has been proposed as a potential vector candidate for specific gene expression in pain-related dorsal root ganglion (DRG) neurons, but this has not been confirmed in nonhuman primates. The aim of our study was to analyze the transduction efficiency and target specificity of this viral vector in the common marmoset by comparing it with those in the rat. When green fluorescent protein-expressing serotype-6 vector was injected into the sciatic nerve, the efficiency of gene expression in DRG neurons was comparable in both species. We found that the serotype-6 vector was largely specific to the pain-related ganglion neurons in the marmoset, as well as in the rat, whereas the serotype-9 vector resulted in contrasting effects in the two species. Neither AAV6 nor AAV9 resulted in DRG toxicity when administered via the sciatic nerve, suggesting this as a safer route of sensory nerve transduction than the currently used intrathecal or intravenous administrative routes. Furthermore, the AAV6 vector could be an optimal serotype for gene therapy for human chronic pain that has a minimal effect on other somatosensory functions of DRG neurons.

INTRODUCTION

For the treatment of chronic pain, one potent therapeutic possibility is to transfer genetic molecules into the peripheral sensory nervous system to manipulate nociceptive physiology.^{1–5} Although a number of pharmacological molecules have been reported to have potential to modulate sensory neuron function in chronic pain,^{6,7} a feasible delivery system of these molecules to appropriate neurons in peripheral sensory afferents has yet to be established; this would be a pivotal step toward translating effective gene therapy into human chronic pain research.

The adeno-associated virus (AAV) vector is now considered one of the most useful vectors for gene therapy owing to their minimal immunogenicity and toxicity.⁸ Gene delivery into dorsal root ganglion (DRG) neurons has been proven possible^{9,10} by using an AAV vector, and more importantly, distinct serotypes of AAV vectors

have been shown to possess different cellular tropisms.¹¹ This target specificity is potentially advantageous, especially for gene delivery into DRG neurons because of their heterogeneous nature; DRG neurons comprise different classes of neurons, which have distinct sensory modalities, such as tactile sense and proprioception, along with nociception.^{12–17} Indeed, several studies have reported the successful delivery of foreign genes into each class of neurons, with relatively high specificity. Importantly, the AAV6 vector has been shown to display a higher level of gene transduction into DRG neurons with small-diameter nociceptive afferents.^{18–21} However, other serotypes of AAV vectors exhibit different target specificity to DRG neurons. For example, AAV8 and AAV9 vectors have been reported to be effective in delivering genes into large-diameter DRG neurons^{22,23} that signal deep muscle and tactile sensations, but not nociception. Furthermore, by taking advantage of the target specificity of AAV vectors, the use of optogenetics to selectively modulate nociceptive,^{20,21,24–26} as well as non-nociceptive,^{23,26} DRG neuron activity has also been reported. Similarly, sustained relief of chronic pain has been achieved in a rodent model, by target-selective delivery of calcium ion (Ca²⁺) channel-related peptides, together with the AAV6 vector.²⁷

Distinct target specificity of AAV vectors to DRG neurons warrants their translational application. For example, if a comparable specificity can be confirmed in human patients, pain could be modulated using an AAV6 vector. However, to date, this target specificity has not been investigated in nonhuman primates. Indeed, most recent comparable approaches in monkeys^{28–31} addressed the target specificity of AAV vectors to brain tissue, but not to the peripheral nervous system. As for peripheral neural structures, successful gene delivery by AAV7 or AAV9 vectors into a variety of neurons, including DRG

Received 2 September 2020; accepted 27 July 2021;
<https://doi.org/10.1016/j.omtm.2021.07.009>.

Correspondence: Kazuhiko Seki, Department of Neurophysiology, National Institute of Neuroscience, National Center of Neurology and Psychiatry, Kodaira, Tokyo, Japan.

E-mail: seki@ncnp.go.jp



neurons, has been achieved by intrathecal^{32,33} or intravascular application.^{34,35} Nevertheless, the target specificity within DRG neurons has not been reported previously. The higher cellular tropisms of the AAV6 vector to small-diameter nociceptive afferents and the AAV9 vector to large-diameter DRG neurons are currently restricted to rodent models, and thus cannot be generalized to either nonhuman primates or humans.

The aim of our study was to examine whether the target specificity of AAV6 and AAV9 vectors to DRG neurons that relay nociceptive or other somatosensory signals, respectively (as established in rodent models^{18–23}), can be reproduced in nonhuman primates. We injected each of the vectors into the sciatic nerve in both the rat and common marmoset (a New World monkey) and compared their target specificity within DRG neurons.

RESULTS

Eight young male Jcl:Wistar rats (4 weeks old) and 12 adult common marmosets of either sex (four males and eight females) were used. Comparable experimental designs were applied for both rats and marmosets: they were each split into two groups, and the efficiency of gene transduction was compared for the AAV6 and AAV9 vectors.

In both the rat and marmoset, we found vigorous fluorescence in the ipsilateral sciatic nerve, DRGs, and spinal cord 4 weeks after vector injection (Figure 1). This suggested that gene transfer to these regions was successfully achieved via anterograde transport from the sciatic nerve injection (Figures 1A and 1B). We observed stronger fluorescence in the segments of L4 and L5 in the rat (Figures 1C and 1D) and of L5 to L7 in the marmoset (Figures 1E and 1F). This difference in the segmental distribution is considered reasonable for the species difference in sciatic nerve anatomy.³⁶ In the spinal cord, we found strong expression of green fluorescent protein (GFP) not only in the DRGs, but also in the dorsal lemniscus (Figures 1C–1F), where the proximal axon of DRG cells ascend toward the brainstem. However, limited fluorescence was observed for DRGs that did not accommodate sciatic nerve afferents (e.g., contralateral DRGs). This result indicated a lower off-target effect for intra-nerve induction.

We further confirmed DRG-cell specific transduction of the exogenous GFP gene by quantification of the vector genome copy number (VGCN). First, we analyzed the VGCN of the spinal cord in all rats ($n = 8$) and marmosets ($n = 12$). Two slices of the lumbar spinal cord were analyzed for each animal: one with vigorous GFP-positive fluorescence (GFP⁺; L3 to L5) and another with little fluorescence (GFP⁻; L1 to L3). The VGCN of the skeletal muscle innervated by the sciatic nerve (MG) and its antagonist (TA) was also analyzed in the marmosets ($n = 8$). Results are summarized in Figure 1G. We've found a significant difference in copy number between the spinal samples of GFP⁺ and GFP⁻ in the marmoset (0.58 ± 0.59 versus 0.03 ± 0.03 , $p < 0.01$, Student's *t* test) and the rats (0.62 ± 0.50 versus 0.16 ± 0.16 , $p < 0.05$, Student's *t* test). Second, we've

found almost zero copy in either the MG or TA muscles (0.01 ± 0.01 versus 0.002 ± 0.002 , $p > 0.05$, Student's *t* test). As shown in Figure 1, these results demonstrated that expression of GFP was highly specific to DRGs, as well as to the spinal segments that innervated the nerve where the virus vector was injected, but without the off-target effect on tissues surrounding the site of injection (i.e., the muscles). Figures 2A–2D show examples of immunostained sections containing DRG neurons transduced by AAV6 (A and C) and AAV9 (B and D) vectors in the rat (A and B) and marmoset (C and D). We immunostained with the antibodies, GFP (green) and neuron-sensitive marker (NeuN; red), to confirm successful gene delivery into DRG neurons. In these examples, we found a specific difference between the rat and marmoset. In the rat, the DRG neurons transduced by the AAV9 vector seemed to be larger than those transduced by the AAV6 vector. However, in the marmoset, this contrast was less dominant.

Next, by applying immunofluorescence histochemistry as shown in Figures 2A–2D, we compared the transduction efficacy into DRG neurons between the rat and marmoset. Specifically, we were interested in the extent to which the two AAV vectors can transduce the GFP gene into DRG neurons in the rat and marmoset. To this end, we counted the number of GFP⁺ neurons among the NeuN⁺ DRG neurons (GFP⁺NeuN⁺; 487.7 ± 221.0 for rats and 535.1 ± 187.5 for marmosets) and calculated the percentage of GFP⁺NeuN⁺ neurons in NeuN⁺ neurons. As shown in Table 1, we found similar characteristics of transduction efficiency in both the rat and the marmoset. For example, the efficiency by the AAV9 vector in the rat was 30.03% on average (i.e., approximately one-third of the DRG neurons in each segment showed GFP⁺NeuN⁺) and that in the marmoset was 30.83%; there was no significant difference between the two species (Wilcoxon rank sum test, $p = 0.61$). The efficiency by the AAV6 vector was 21.24% in the rat and 18.93% in the marmoset, which were not significantly different (Wilcoxon rank sum test, $p = 0.71$). In addition, we found no statistically significant difference in the transduction efficiency between the AAV6 and AAV9 vectors in either the rat or the marmoset (Wilcoxon rank sum test, $p = 0.31$ and $p = 0.70$, respectively). Therefore, we conclude that in general, the transduction efficacy of these vectors into DRG neurons does not differ between the marmoset and the rat.

We then compared the target specificity of the AAV6 and AAV9 vectors in the rat and marmoset. Representative examples are shown in Figures 2E–2L. For this analysis, we stained each DRG slice for NF200, a marker for myelinated primary afferents and DRG cells that convey somatosensory signals other than nociception,³⁷ and peripherin, a marker for unmyelinated primary afferents and DRG cells that convey nociceptive signals.³⁸ Subsequently, we counted the DRG cells that exhibited double labeling for both GFP and NF200 or peripherin.

In the rat, we confirmed the specificity for nociceptive- and other somatosensory-related DRG neurons, as reported previously.^{18–23} For

www.moleculartherapy.org

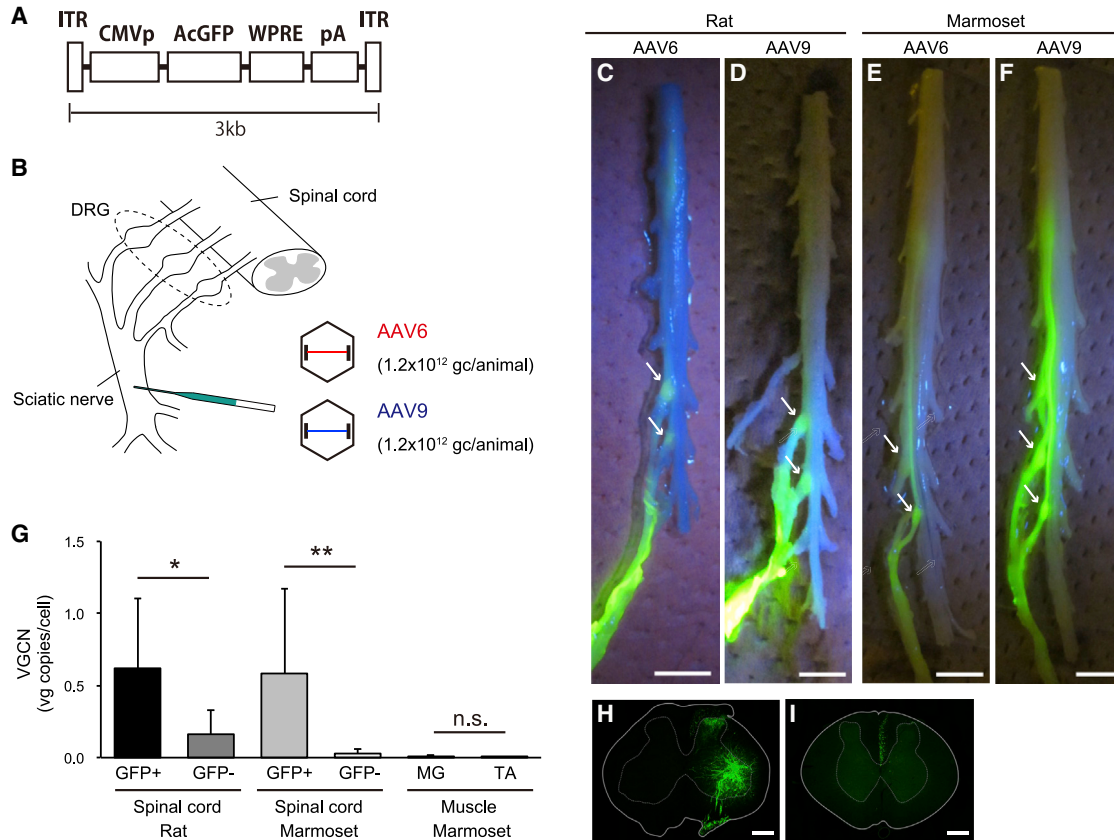


Figure 1. Intra-nerve injections of AAV-GFP vectors in the rat and marmoset

(A) Schematic representation of the AAV vector constructs. AcGFP is expressed under the control of the CMV promoter. ITR, inverted terminal repeat; WPRE, woodchuck hepatitis virus post-transcriptional regulatory element. (B) Illustrations of the method to inject AAV6-GFP and AAV9-GFP vectors in the rat and marmoset. Gene transfer of the AAV vectors into DRG neurons was achieved by anterograde transport through their axons after vector injections into the proximal part of the left sciatic nerve in the rat and marmoset. The sciatic nerve predominantly innervates L4 to L6 DRGs in the rat and L5 to L7 DRGs in the marmoset (ellipse dashed line). The pattern of gene transduction into DRG neurons was analyzed in these segments. (C–F) Example of a GFP fluorescence image of the spinal cord with the DRGs and sciatic nerve in the rat and marmoset with the AAV6-GFP and AAV9-GFP vectors injected. White arrows indicate the lumbar DRGs expressed GFP at 4 weeks after vector injection. (G–I) Vector genome copy number (VGCN) assessment to lumbar spinal cord and muscles surrounding the sciatic nerve. (G) Results of VGCN assessments for the spinal cord of the rat, marmoset, and for the skeletal muscles of the marmoset. GFP⁺, a slice of spinal cord segment receiving (thus exhibiting a dominant fluorescence, H) or not receiving (thus exhibiting little fluorescence, I) afferents from the sciatic nerve. MG, medial gastrocnemius muscles; TA, tibialis anterior muscles. (H and I) Representative spinal cord sections showing GFP expression (green) in L5 (H) and L2 (I) segments in the same marmoset. Data are presented as mean \pm standard deviations * $p < 0.05$, ** $p < 0.01$, Student's *t* test. Scale bars, 1 cm for (C)–(F), 50 μ m for (H) and (I).

example, in the case of AAV6 vector injection, GFP⁺ cells were found to be more frequently co-labeled for peripherin (Figures 2F–2F'') than for NF200 (Figures 2E–2E''; compare arrows in Figures 2E'' and 2F''). Conversely, in the case of AAV9 vector injection, the co-labeled cells were found more often for NF200 (Figures 2G–2G'') than for peripherin (Figures 2H–2H''; compare arrows in Figures 2G'' and 2H''). Therefore, we successfully reproduced the previous findings in rodents.^{18–23} This confirmation is further supported by the transduction efficiency results (expressed as the ratio of NF200- or peripherin-labeled cells to GFP-labeled cells; Figure 2M, left and 2N, left). We found that the AAV6 vector exhibited higher transduction efficiency into DRG neurons with unmyelinated fibers (peripherin labeled, Wilcoxon rank sum test, $p < 0.05$) and the AAV9 vector showed higher

efficiency into DRG neurons with myelinated fibers (NF200 labeled, Wilcoxon rank sum test, $p < 0.05$).

A primary question for this study was whether the comparable target specificity of the AAV vectors to DRG neurons found in the rat is also represented in the marmoset. To address this issue, we repeated the equivalent examination in the marmoset and revealed two findings. First, in the case of AAV6 vector injection, we found that a proportion of the double-labeled cells was observed within peripherin-labeled cells (Figures 2J–2J'') more frequently than within NF200-labeled cells (Figures 2I–2I''). This profile was similar to the findings in the rat (Figures 2E–2F''). Further population analysis of the transduction efficiency of the AAV6 vector (Figure 2M, right) confirmed that the

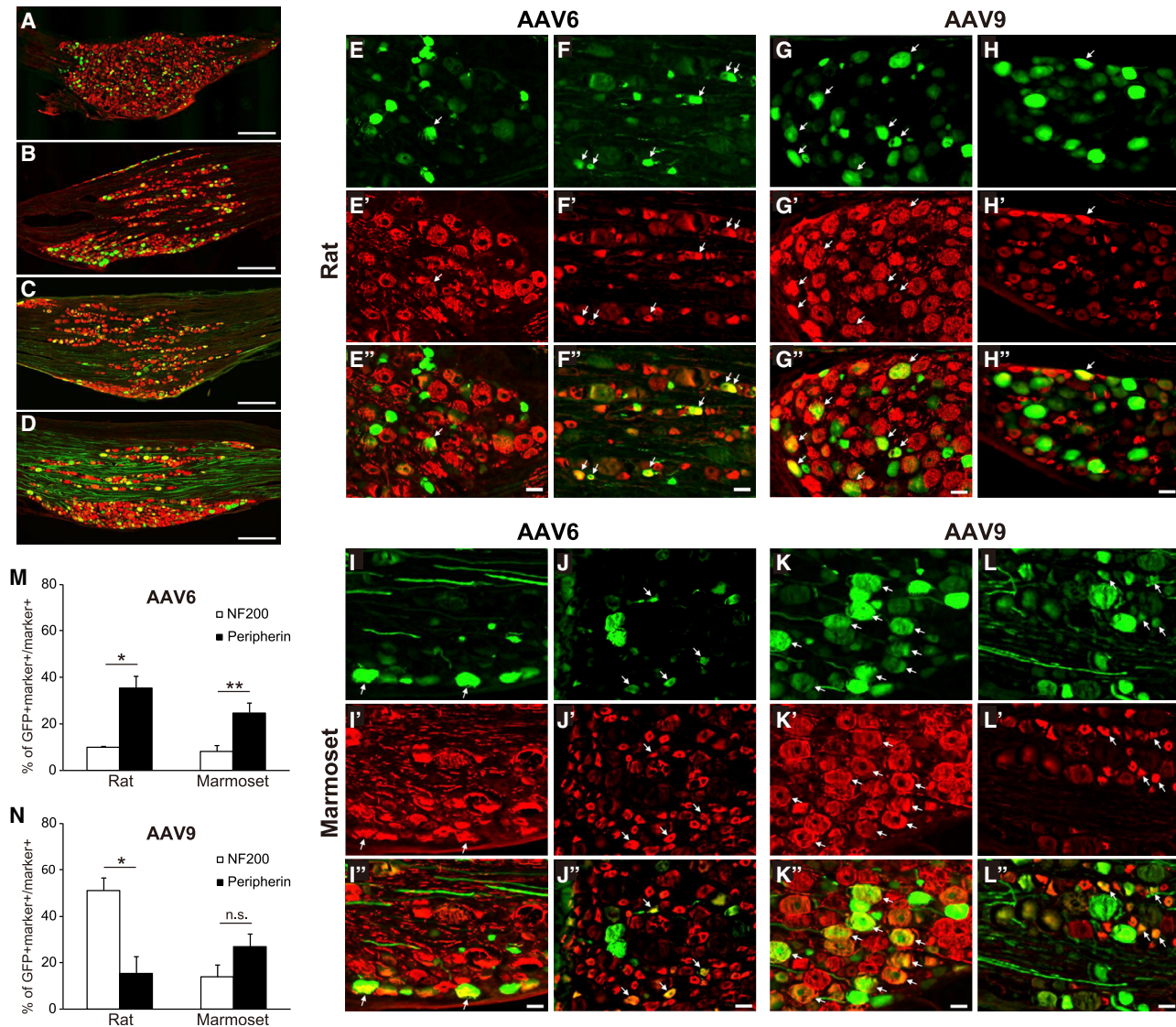


Figure 2. Immunohistochemical evaluation and target-specific gene expression in DRG neurons in the rat and marmoset

(A–D) DRG sections stained 4 weeks after the sciatic nerve injections of AAV6-GFP (A and C) and AAV9-GFP (B and D) vectors in the rat (A and B) and marmoset (C and D). Each section was immunostained with antibodies of GFP (green) and NeuN (red). Note that yellow/orange cells represent co-expression of GFP and NeuN. Scale bars, 500 μ m. (E–L) Representative DRG sections from the rat (E–H) and marmoset (I–L) processed for immunofluorescence histochemistry for GFP and markers for neuronal subpopulations, NF200 (marker for myelinated [somatosensory, other than nociceptive] primary afferents and DRG cells), and peripherin (marker for unmyelinated [nociceptive] primary afferents and DRG cells). Arrows indicate neurons co-expressed with GFP and cell type markers. Note that the glial cells (e.g., satellite cells) were not counted (see [Materials and methods](#)). Scale bars, 50 μ m. (M and N) Probability of the co-expression of NF200 (open bar) or peripherin (filled bar) in GFP⁺ neurons in the rat and marmoset. Data are presented as means \pm SEM. * $p < 0.05$, ** $p < 0.01$, Wilcoxon rank sum test. Note that serotype 6 exhibited high specificity to peripherin⁺ neurons in both the rat and marmoset, whereas serotype 9 displayed specificity to NF200⁺ neurons in the rat, but not in the marmoset.

target specificity of the AAV6 vector was biased toward peripherin-over NF200-labeled DRG neurons in both the rat and marmoset. Therefore, this result indicates that the target specificity of the AAV6 vector is represented in nonhuman primates, as well as in rodents. Second, we found that the target specificity of the AAV9 vector in the marmoset was different from that in the rat. For example, the GFP transduction by AAV9 vector did not exhibit high preference to

NF200-labeled cells, as was the case in the rat (compare [Figures 2G''](#) and [2H''](#)). Instead, we found a comparable number of NF200-labeled ([Figures 2K''–2K'''](#)) and peripherin-labeled ([Figures 2L''–2L'''](#)) cells (compare [Figures 2K''](#) and [2L''](#)) in the marmoset. Again, these results were supported by a population analysis ([Figure 2N](#)): Although the AAV9 vector exhibited higher specificity to the NF200-labeled cells in the rat, the efficiency of transduction did not differ in the

Table 1. Experimental summary

| Serotype | Animal | Number of animals | NeuN ⁺ cells | GFP ⁺ NeuN ⁺ cells | GFP ⁺ NeuN ⁺ /NeuN ⁺ (%) |
|----------|----------|-------------------|-------------------------|--|---|
| AAV6 | rat | 4 | 421.0 ± 123.1 | 92.5 ± 49.1 | 21.24 |
| AAV6 | marmoset | 6 | 556.3 ± 369.0 | 143.8 ± 181.2 | 18.93 |
| AAV9 | rat | 4 | 554.5 ± 294.8 | 163.5 ± 96.1 | 30.03 |
| AAV9 | marmoset | 6 | 514.0 ± 337.1 | 231.3 ± 310.7 | 30.83 |

Data are presented as means ± standard deviations.

NF200- and peripherin-labeled cells in the marmoset (Wilcoxon rank sum test, $p > 0.05$).

To confirm whether these observations might be influenced by potential immune cell infiltration,^{33,39,40} we examined the immune responses of DRG cells by histological examination of hematoxylin and eosin (H&E)-stained DRG sections in both the rat and marmoset (Figure 3). We found little sign of cellular infiltration in the AAV-9 injected (A–C), the AAV-6 injected (D–F), and the control animals (G and H). We found satellite cells or lymphocytes in every section, but they were not at the level of differentiating into macrophages, and we found no significant difference between the AAV-injected and control DRGs. We found no sign of cellular degeneration that is commonly observed when the AAV vector is administered via blood or cerebrospinal fluid.⁴⁰ Therefore, we concluded that the AAV vectors applied via the intra-nerve route at the current titer (1.2×10^{12} gc/6 μ L/animal) did not have their own toxic effects on DRG neurons.

Overall, we found that although the AAV6 vector displayed a comparable degree of target specificity (i.e., biased toward peripherin-labeled cells) in both the rat and marmoset, no clear target specificity of the AAV9 vector was detected in the marmoset, unlike in the rat, which showed specificity biased toward NF200-labeled cells.

This conclusion was further confirmed by the axonal projection pattern of primary afferents in the spinal cord (Figure 4). For this analysis, we compared the intraspinal, topological pattern of axonal projection revealed by AAV6 (Figures 4D–4K) and AAV9 (Figures 4L–4S) vectors in the rat (Figures 4D–4G and 4L–4O) and marmoset (Figures 4H–4K and 4P–4S), respectively. As expected from the peripherin-labeled cell preference in both the rat (Figures 2F–2F”) and marmoset (Figures 2J–2J”), we found that the projection from AAV6-labeled axons mostly terminated within the superficial layers of the dorsal horn (lamina I and outer lamina II), where co-labeling was found prominently with calcitonin gene-related peptide (CGRP, a marker for unmyelinated [nociceptive] peptidergic afferents;^{19,41} Figure 4E) and, to a lesser extent, with vesicular glutamate transporter 1 (VGLUT1, a marker for myelinated [somatosensory other than nociceptive] primary afferents;⁴² Figure 4F). Indeed, when we compared Figures 4E and 4I, the cells co-labeled for both CGRP and GFP were clustered in lamina I and II in both the rat and marmoset. This supports our conclusion that in both rodents and nonhuman primates, the AAV6 vector possesses relatively higher specificity for transduction into the noxious, probably pain-related,

fibers. However, we found a highly contrasting result for the AAV9 vector. In the rat, the proximal axons of DRG neurons traveled beyond the superficial layers of the dorsal horn, where some neurons were co-labeled with VGLUT1 (Figure 4N). Some of them reached an area proximal to the ventral motor neuron pool (Figure 4O), which suggested that they were group I, large-diameter, somatosensory afferents. Conversely, the pattern of intraspinal labeling for the AAV9 vector in the marmoset was comparable to that for the AAV6 vector; the projection was restricted to the superficial dorsal horn, which was co-labeled with CGRP but not with VGLUT1. This observation supports our suggestion that the target specificity of the AAV vectors is different in rodents and nonhuman primates, depending on the serotype of the vectors.

To supplement these findings, we found that AAV6^{43,44} and AAV9^{32,45} vectors can label motor neurons in the ventral horn via retrograde transduction in the sciatic nerve (Figures 4G, 4K, 4O, and 4S). We found no systematic differences in either the transduction efficacy or the target specificity to the motor neurons as shown in Figure 4. Improving the transduction efficacy and target specificity to avoid the off-target effect on spinal motor neurons are also important issues to test in nonhuman primates in future studies.

DISCUSSION

The primary motivation of the present study was to examine whether the target-specific gene transduction into DRG neurons (nociceptive and other somatosensory afferents) by different AAV vector serotypes (6 and 9) that has been well established in rodent models might be reproducible in a nonhuman primate model. We compared the efficiency of gene transduction into DRG neurons and the lumbar segments of the spinal cord in rodents and common marmosets and obtained two novel findings. First, we found that the target specificity of the AAV6 vector to DRG neurons with noxious, non-myelinated afferents in the marmoset was comparably high to that in rat. Second, the target specificity of the AAV9 vector to DRG neurons with myelinated afferents observed in the rat was not reproduced in the marmoset. These findings indicate that the AAV6 vector is a suitable AAV serotype for gene therapy in patients who suffer from chronic peripheral pain. However, our results also suggest that the target specificity common to rodents and nonhuman primates does not apply to all serotypes of AAV vectors or subpopulations of DRG neurons, and further exploration will be required before developing AAV-mediated gene therapy for restoring somatosensory functions via selective transduction into DRG neurons that convey proprioception and tactile signals.

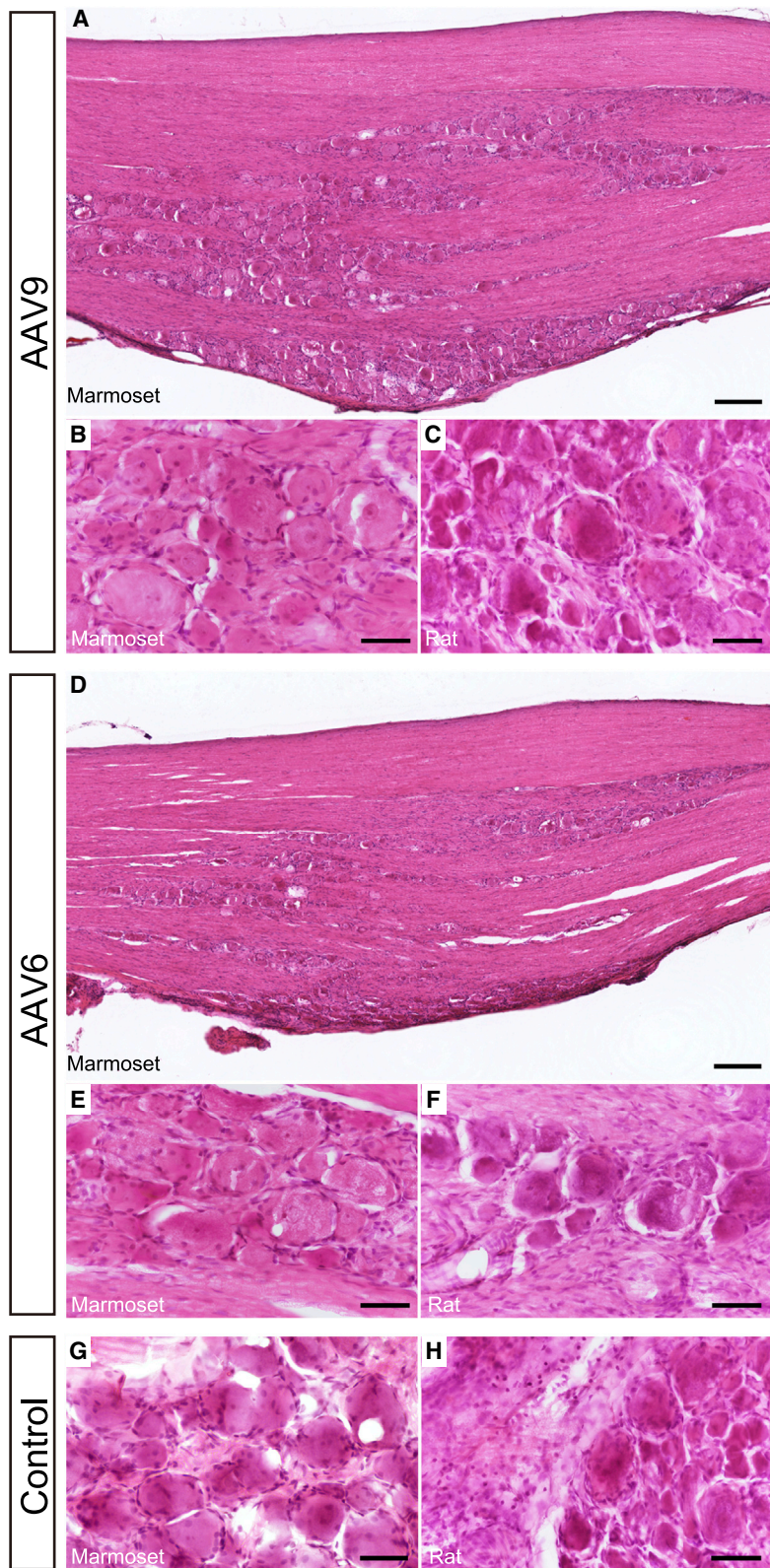


Figure 3. H&E-stained DRG sections

Hematoxylin and eosin (H&E)-stained DRG sections stained 4 weeks after the sciatic nerve injections of AAV9-GFP (A–C), AAV6-GFP (D–F) vectors, and control (G and H) in the marmoset (A, B, D, E, and G) or rat (C, F, and H) segments. Representative examples from L4 (C and F) or L5 (A, B, D, E, G, and H) segments. Scale bars, 200 μm for (A) and (D) and 50 μm for (B), (C), and (E)–(H).

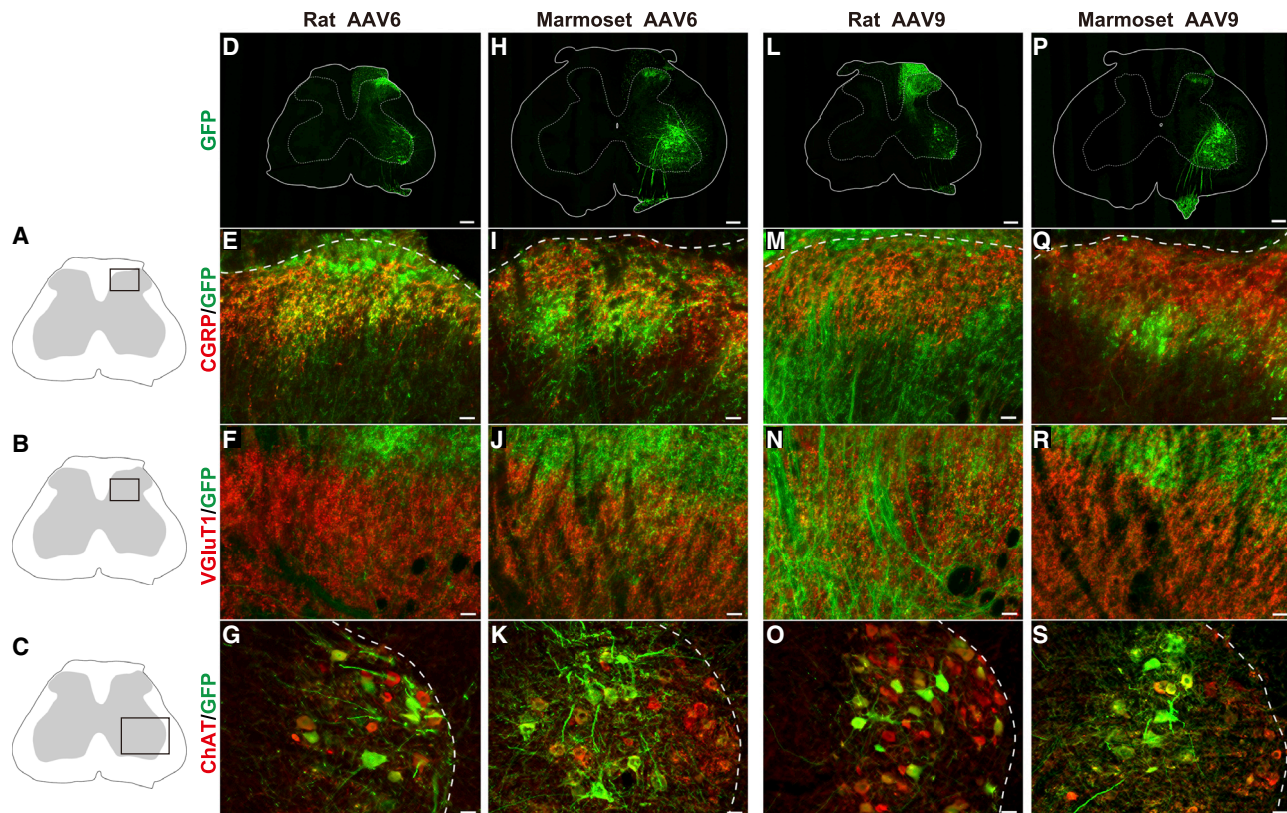


Figure 4. Expression of GFP in the spinal cord of the rat and marmoset

(D, H, L, and P) Representative low-power magnification images of transverse spinal cord sections at the L4 (rat) and L6 (marmoset) lumbar levels showing GFP expression (green) 4 weeks after the AAV6-GFP and AAV9-GFP vector injections. White lines indicate transverse section profiles of the spinal cord, and white broken lines denote gray matter. (E–G, I–K, M–O, and Q–S) High-power magnification of the rectangular areas in (A) E, I, M, and Q, (B) F, J, N, and R, and (C) G, K, O, and S. These images demonstrate co-expression of GFP (green) with CGRP (a marker for unmyelinated [nociceptive] peptidergic afferents; red; E, I, M, Q), VGlut1 (a marker for myelinated [somatosensory other than nociceptive] primary afferents; red; F, J, N, R) in the dorsal horn, or ChAT (a marker for motor neurons; red; G, K, O, S) in the ventral horn for the AAV6-GFP and AAV9-GFP vectors. White broken lines denote the dorsal and ventral horns. Scale bars, 250 μ m for (D), (H), (L), and (P); 25 μ m for (E)–(F), (I)–(J), (M)–(N), and (Q)–(R); and 50 μ m for (G), (K), (O), and (S).

AAV6 vector as a superior serotype for pain-modulating gene therapy

In rodents, the AAV6 vector possesses a high level of gene transduction into DRG neurons with small-diameter nociceptive afferents.^{18–21} By taking advantage of its target specificity, the AAV6 vector is effective for its application in the treatment of neuropathic pain. For example, the use of the AAV6 vector for delivering the CDC3 peptide, thought to be a potential peptide for pain management⁴⁶ by activating a voltage-gated Ca^{2+} channel blocker,⁴⁷ has been shown to effectively prevent the development of cutaneous mechanical hypersensitivity in a rat neuropathic pain model²⁷ and in established neuropathic pain in rats.⁴⁸ In a similar vein, the attenuation of neuropathic pain using an AAV6 vector was also achieved by delivering an interfering peptide of transient receptor potential vanilloid 1.⁴⁹ Furthermore, the effectiveness of gene transduction by an intraspiically applied AAV6 vector has been demonstrated to express opsins in nociceptors and successfully suppress pain responses in mice through optogenetics²⁰ and chemogenetics.²¹ Remarkably, a therapeutic effect was achieved by the trans-

duction of opsin into only 16.5% of all DRG neurons,²⁰ which is lower than the transduction rate in our work (see Figure 2M). Therefore, our observation of comparable transduction efficiency of the AAV6 vector into DRG neurons with unmyelinated, nociceptive afferents in the rat and marmoset will pave the way to translate this prospective treatment for chronic pain into nonhuman primates and, eventually, into human patients.

Another advantage of AAV6-mediated gene transduction into DRG neurons is the low off-target effect. We found that expression of GFP was largely limited (9.99% in the rat and 8.06% in the marmoset) in DRG neurons with myelinated afferents (i.e., NF200⁺ cells), whereas a higher transduction efficiency was seen in DRG neurons with unmyelinated afferents. In fact, this was the lowest transduction efficiency among all marker (NF200 or peripherin) and serotype (AAV6 or AAV9) combinations (Figures 2M and 2N). An off-target issue may be a major disadvantage⁵⁰ for AAV-mediated gene expression in the nervous system. Therefore, this low off-target effect would

be beneficial to the translation into pain management therapy, considering the heterogeneous nature of DRG neuron populations. Indeed, the low off-target effect of the AAV6 vector could allow us to suppress^{20,21,27,48} the excitability of noxious, pain-related DRG neurons with minimal effects on other somatosensory functions.

Enhanced target specificity and safety by intra-nerve injection

Our results showed that intra-nerve injection for gene expression in noxious, pain-related DRG neurons manifests unique properties of high target specificity and low off-target effects of the AAV6 vector. In the past, gene transfer into DRG neurons has been reported using numerous delivery routes other than the intra-neural method, such as subcutaneous, intramuscular, intravenous, intrathecal, and intraganglionic routes.^{18,19,22,51,52} Among these, the intraganglionic route enables the most efficient gene expression in a spinal segment with no obvious off-target effects.⁹ However, with regard to its clinical application to human patients, direct DRG injection is disadvantageous because of the risk of damaging DRG neurons during the highly invasive procedure to expose the DRG injection site.^{53,54} Recently, the intravenous route has drawn attention since the discovery of an AAV variant with superior transduction efficacy in a wide range of neurons in the central nervous system (CNS).^{55,56} However, intravenous administration, alongside the all-systemic route, has obvious limitations when aiming to further target specificity among the considerably heterogeneous DRG neuronal populations. To take advantage of the superiority of systemic administration,^{55,56} we require the development of a promoter that is specific to noxious, pain-related DRG neurons that have been previously developed for rodents.⁵⁷ Although a promoter specific to marmoset neurons has recently been developed,^{58,59} one that is specific to DRG neurons is not yet available.

In addition, a number of studies have recently reported toxicity of intravenously administered AAVs in DRG neurons.^{60–62} For example, Hordeaux et al.⁴⁰ reported that intravenous or intra-cisterna magna administration of AAV9 to non-human primate result in severe DRG pathology 3 weeks after the injection. In contrast, we found no sign of toxicity to AAV9 application even at 4 weeks after the injection via the intra-nerve route (Figure 3). Therefore, we propose that intra-nerve injection, with the aid of the AAV6 vector's higher tropism and lower off-target nature, is an optimal and safe approach to gene therapy for pain relief in humans.

Different DRG target specificity of AAV9 vector in rodents and nonhuman primates

We found different target specificity to DRG neurons in AAV9-mediated gene delivery between the rat and marmoset. Although there was preferential transduction into the cells with myelinated afferents in the rat, this was less clear in the marmoset. In fact, there was a tendency for bias toward transduction into the cells with unmyelinated afferents (Figure 2N).

The mechanism underlying the differential target specificity of the AAV9 vector in the rat and marmoset is unclear, though the spectrum of cellular tropism of different AAV serotypes to subtypes of DRG

neurons may differ in the two species. For example, AAV1 and AAV5 vectors showed higher transduction efficiency for both large- and small-diameter (isolectin B4⁺ [IB4⁺] and CGRP⁺) DRG neurons,¹¹ suggesting their wider spectrum of cellular tropism. Conversely, a specific serotype may have a narrower spectrum and more distinct preference for specific DRG neurons. For instance, the AAV6 vector achieved a high level of gene transduction into DRG neurons with small-diameter nociceptive afferents.^{18–21} In contrast to the AAV6 vector, AAV8 and AAV9 vectors were highly effective in delivering genes into large-diameter DRG neurons.^{22,52} It is reasonable to assume that these spectra of cellular tropism that have so far been established only in the rodent are different in primates. We found comparable efficacy of the AAV6 vector in the rat and marmoset, which indicated that nociceptive DRG neurons in both species may have similar spectra of tropism among different AAV serotypes. However, we also observed a distinct level of gene transduction efficacy of the AAV9 vector into DRG cells with myelinated afferents. This suggests that the spectrum of cellular tropism to somatosensory afferents differs in rodents and nonhuman primates. If so, it raises the possibility that serotypes other than AAV6 and AAV9 may have higher tropism to this specific type of DRG neuron exclusively in nonhuman primates. This would need to be confirmed in a future study.

One may argue that both the AAV9 and AAV6 vectors could be suitable candidates for chronic pain treatment based on our observation of comparable transduction efficacy to nociceptive DRG neurons. However, recent reports contradict this possibility. In the piglet, a high systemic dose of the AAV9 vector caused proprioceptive deficits and ataxia,⁶⁰ which clearly indicates that the AAV9 vector has high transduction into myelinated DRG afferents. In the marmoset, an intravenous injection of the AAV-PHP.B vector, a variant of the AAV9 vector, resulted in high transduction into DRG neurons projecting to the medulla oblongata.³⁵ This also suggests high transduction capacity of the AAV9 vector into myelinated DRG afferents. Because transduction into myelinated DRG neurons is an obvious off-target effect, the use of AAV9, instead of the AAV6 vector, may not be a reasonable choice for application in pain treatment.

Methodological considerations

The age of the rats used in our study was 4 weeks, which was before the sexual maturation age (6 weeks), whereas that of the marmosets ranged between 1.5 and 7.6 years, which was after the sexual maturation age (1.5 years).⁶³ Indeed, the differential target specificity to the same AAV serotypes at different ages of animals has been reported.^{45,64} In nonhuman primates, intravascular administration of the AAV9 vector in neonatal⁶⁵ or juvenile⁶⁶ animals yielded different efficacy of gene transduction into CNS neurons. Therefore, it is possible that some serotypes of AAV vectors (e.g., AAV9) may be sensitive to the age of the animals, whereas others (e.g., AAV6) may not be. Related to the age difference, body weight was also different between the rats and marmosets (see [Materials and methods](#)). Although we confirmed that the virus titer per body weight at the end of each experiment was not different between the rats and marmosets, it is

www.moleculartherapy.org

likely to be different at the time of injection because of the large difference in their body weight. Therefore, we cannot rule out the possibility that the distinct virus titers at the early phase of viral infection affected our findings to some extent.

Finally, the cytomegalovirus (CMV) promoter is susceptible to silencing,⁶⁷ which results in decreased recombinant protein production.⁶⁸ The CMV promoter has been shown to drive transgene expression in DRG neurons for up to 12 weeks *in vivo*.^{9,11,18,19,22} Nevertheless, it is possible that the lower rate of gene expression in our study (i.e., myelinated DRG neurons transduced with the AAV6 vector in both the rat and marmoset and with the AAV9 vector in the marmoset, and the unmyelinated DRG neurons transduced with the AAV9 vector in the rat) was affected by variation in silencing among the species and/or cell types. To address this issue, further investigations are needed; for example, by analyzing genome copy numbers for individual subpopulations of DRG neurons in different species.

MATERIALS AND METHODS

Experimental animals

Twelve adult common marmosets (1–8 years old) of both sexes (four male and eight female) and eight young male Jcl:Wistar rats (4 weeks old) were used. Body weight at the day of sacrifice was 337.99 ± 36.11 g for marmosets and 286.13 ± 26.83 g for rats. Animals were housed under standard conditions with food and water *ad libitum* and a 12-h:12-h light:dark cycle. All experiments were conducted in accordance with protocols approved by the Ethics Committee for animal research of the National Institute of Neuroscience, NCNP, Japan.

Production of viral particles

AAV-CMV-AcGFP vector serotype 6 (2.00×10^{14} genome copies mL^{-1}) and 9 (2.00×10^{14} genome copies mL^{-1}) were produced by the helper-free triple transfection procedure and purified using CsCl gradient or affinity chromatography (GE Healthcare). Viral titers were determined by quantitative PCR using TaqMan technology (Life Technologies, Gaithersburg, MD, USA). The purity of the vectors was assessed by 4%–12% sodium dodecyl sulfate-acrylamide gel electrophoresis and fluorescent staining (Oriole, Bio-Rad, Hercules, CA, USA). The transfer plasmid (pAAV-CMV-AcGFP-WPRE) was constructed by inserting an AcGFP fragment with the WPRE sequence into an AAV backbone plasmid (pAAV-CMV, Stratagene).

Virus injection

Rats were anesthetized with an intraperitoneal injection of pentobarbital sodium (30 mg/kg) and an intra-muscular injection of butorphanol (0.1 mg/kg). Adequate anesthesia depth was monitored frequently by checking the pupil size and flexion reflex to paw pinch. To expose the sciatic nerve for the injection, we fixed rats in a prone position and the left leg was shaved up from the thigh to the spine. We cut the skin over the gluteus muscles and made a blunt dissection to separate both heads of the biceps femoris. Once the sciatic nerve was detected below the biceps femoris, we further exposed the nerve proximally until it entered the greater sciatic notch. The total length of the exposed sec-

tion of the sciatic nerve was approximately 2 cm from the sciatic notch. The exposed nerve was isolated from the surrounding tissues and then covered with wet cotton to keep the nerve moist for the prospective injection.

The virus injections (Figures 1A and 1B) were performed with a glass capillary (0.6/1.0 mm internal/external diameters; Narishige, Japan) pulled to a fine point and attached with a polyethylene tubing (JT-10, EICOM, Kyoto, Japan) to a Hamilton syringe (1702RN, GL Science, Japan) that was mounted onto a microinjection pump (NanoJet Quasi-S, ISIS, Seoul, South Korea). The tubing, syringe, and capillary were filled with an electrically insulating stable fluorocarbon-based fluid (Fluorinert, 3M, St. Paul, MN, USA). We added 1% Fast Green (1 μL) to the viral vector solution to visualize the injected solution. The tip of the glass capillary was inserted into the sciatic nerve 10 mm distal to the greater sciatic foramen. After a 5-min delay to allow sealing of the tissue around the glass capillary tip, a 6 μL viral vector solution was injected at a rate of 0.5 $\mu\text{L}/\text{min}$. A dose of 6 μL was injected into both rats and marmosets. The dose was determined according to the results of a brief dose-ranging test using 12 μL (three rats) or 6 μL (one rat) in the pilot study for our previous paper,²³ where we found higher transduction efficacy at a lower dose that was likely due to dose-dependent toxicity. The virus titer per body weight did not differ between the rats and marmosets ($4.83 \pm 1.36 \times 10^{12}$ gc/kg versus $4.00 \pm 1.36 \times 10^{12}$ gc/kg; $p = 0.144$, *t* test). 10 min after the termination of the injection, the capillary was removed. The wound was closed with a non-absorbable suture, and the animals were allowed to recover at 37°C.

Apart from the anesthesia protocol, the virus injection procedure for the marmosets was comparable to the rats. Anesthesia for the marmoset was administrated with an intra-muscular injection of ketamine (20 mg/kg) and xylazine (0.4 mg/kg) and was maintained with inhalation of isoflurane (1.5%–2.5% in oxygen).

Quantification of VGCN

Genomic DNA was extracted and purified from different tissues (i.e., spinal cord sections and muscles) using the NucleoSpin tissue kit (Macherey-Nagel, Düren, Germany). The extracted DNA was analyzed for yield and purity using a NanoDrop One UV/Vis spectrophotometer (Thermo Scientific, Wilmington, MA, USA). Viral genome copy numbers were determined by quantitative PCR using TaqMan technology.

Immunohistochemistry

4 weeks after the injection, the animals were anesthetized with sodium pentobarbital (50 mg/kg)⁶⁹ and perfused transcardially with phosphate-buffered saline (PBS; pH 7.4), followed by 300–400 mL of 4% paraformaldehyde (PFA). Thereafter, the lumbar region of the spinal cord, together with the DRG and sciatic nerve, were sampled (Figures 1C and 1D for rats and marmosets, respectively), post-fixed in 4% PFA overnight at 4°C and transferred to 30% sucrose in PBS at 4°C. DRG sections were cut at 20- μm thickness on a cryostat (Microm HM550, Thermo Fisher Scientific, Waltham, MA) and

mounted on amino silane-coated slides. Spinal cord sections were cut in the coronal plane at 50- μ m thickness on a freezing microtome (REM-710, Yamato Kohki Industrial, Saitama, Japan). After washing three times with PBS, the sections were incubated with PBS containing 2% normal goat serum (NGS) for 1 h at room temperature, followed by incubation with a primary antibody, diluted in 2% NGS and 0.1% Triton X-100 in PBS overnight at 4°C. Then, the sections were washed with PBS three times and incubated with a secondary antibody, diluted in 2% NGS in PBS for 1 h at room temperature. Sections were washed with PBS and covered with a glass coverslip. Control sections were stained using the same protocol but omitting the primary antibodies. All processes were performed in a dark chamber. The primary antibodies were as follows: chicken anti-GFP (Abcam, Cambridge, UK) at 1:1,000, rabbit anti-NeuN (Abcam) at 1:2,000, mouse anti-neurofilament 160/200 (NF200; Sigma Aldrich, N2912, St. Louis, MO, USA) at 1:2,000, rabbit anti-peripherin (Millipore, AB1530, Burlington, MA, USA) at 1:400, guinea-pig anti-VGluT1 (Millipore, AB5905) at 1:1,000, guinea-pig anti-CGRP (Thermo Fisher Scientific, PA1-36017) at 1:2,000, and goat anti-choline acetyltransferase (ChAT; Millipore, AB144P) at 1:100. The secondary antibodies were as follows: goat anti-chicken immunoglobulin G (IgG; Abcam, Alexa488), donkey anti-rabbit IgG (Abcam, Alexa555), goat anti-mouse IgG (Molecular Probes, Alexa555, Eugene, OR, USA), goat anti-guinea-pig IgG (Molecular Probes, Alexa555), and donkey anti-goat IgG (Molecular Probes, Alexa555), diluted at 1:500 for each antibody.

Histological quantification

Fluorescence images were acquired using fluorescent microscopy (BZ-X700, Keyence, Japan) at fixed settings using a 10 \times or 20 \times objective. Image analysis and quantification were performed using image analysis software BZ-X710 (BZ-H3M). For the quantification of transduction efficiency, every tenth DRG section spaced by 200 μ m was selected from the serial sections, and 4–6 sections for rats or 3–8 sections for marmosets were obtained per animal. In each selected section, the number of GFP labeled cells was counted. To ensure we counted the neurons, not the satellite cell, we first counted GFP-labeled cells with a diameter larger than approximately 10 μ m. We then calculated transduction efficiency as the percentage of GFP⁺NeuN⁺ cells in NeuN⁺ cells. It is important to note that the transduction efficacy obtained in this way may be underestimated because high GFP expression may antagonize NeuN expression,²⁸ and some of the neurons may not be immunohistochemically stained with NeuN.⁷⁰ For the quantification of the co-localization of different neuronal markers, we calculated the percentage of respective neuron type marker positive neurons within GFP⁺ neurons and the percentage of GFP⁺ neurons co-labeled with the markers. This analysis was performed in 3–5 sections of the DRG in the rats and 3–4 sections in the marmosets. All other histological quantification methods were comparable between rats and marmosets.

Statistical analysis

The transduction efficiency of GFP⁺ neurons for each AAV serotype was compared using the Wilcoxon rank sum test. The proportion of

GFP⁺ cells in each neural marker (NF200/peripherin) for each AAV serotype was compared using the Wilcoxon rank sum test. The data values are presented as means \pm standard error of the mean (SEM). We considered $p < 0.05$ as significant in all statistical analyses.

Data availability

Data that support the findings of this study are available from the corresponding author upon reasonable request.

ACKNOWLEDGMENTS

The authors would like thank Dr. Daisuke Takahara (Tokyo Metropolitan Institute of Neuroscience) and Mayuko Nakano (Department of Neuroscience, Primate Research Institute, Kyoto University) for technical support, the National Bio-Resource Project - Rat for providing information about the PCR primers for rat genome, Dr. Terumi Nakatani (Department Neurophysiology, NCNP) for advising on the genome copy number analysis, and Drs. Ryoichi Saito and Yuko Kata-kai (Administrative Section of Primate Research Facility, NCNP) for helping with the surgeries and post-surgical animal care in the experiment on marmosets. This work was supported by Grant-in-Aid from the Japan Society for the Promotion of Science (JSPS), grant numbers JP19H01092, 19H05724, 19K21825 (to K.S.), and JP17J05310 (to S.K.), and by research grants from the Japan Agency for Medical Research and Development (JP20dm0307021 to K.I. and JP20dm0207077 to M.T. and K.S.). K.S. and K.I. were funded by the JST Precursory Research for Embryonic Science and Technology Program. S.K. was supported as a Research Fellow of the JSPS.

AUTHOR CONTRIBUTIONS

M.K. and S.W. performed the injection surgery and physiological experiments. S.W. and M.K. performed the histological analyses. K.I. and M.T. developed viral vectors. M.K., M.F., and K.I. performed the quantification of vector genome copy number. M.K. performed the H&E staining, and Y.S. and K.S. evaluated the pathology. K.S. conceived and designed the study and was responsible for the experiment, analysis, and interpretation of the data, as well as manuscript drafting, editing, and revising. All authors contributed to the draft and final versions of this paper.

DECLARATION OF INTERESTS

The authors declare no competing interests.

REFERENCES

1. Beutler, A.S. (2010). AAV provides an alternative for gene therapy of the peripheral sensory nervous system. *Mol. Ther.* 18, 670–673.
2. Glorioso, J.C., and Fink, D.J. (2009). Gene therapy for pain: introduction to the special issue. *Gene Ther.* 16, 453–454.
3. Goins, W.F., Cohen, J.B., and Glorioso, J.C. (2012). Gene therapy for the treatment of chronic peripheral nervous system pain. *Neurobiol. Dis.* 48, 255–270.
4. Handy, C.R., Krudy, C., and Boulis, N. (2011). Gene therapy: a potential approach for cancer pain. *Pain Res. Treat.* 2011, 987597.
5. Guedon, J.M., Wu, S., Zheng, X., Churchill, C.C., Glorioso, J.C., Liu, C.H., Liu, S., Vulchanova, L., Bekker, A., Tao, Y.X., et al. (2015). Current gene therapy using viral vectors for chronic pain. *Mol. Pain* 11, 27.

6. Ogawa, N., Kawai, H., Terashima, T., Kojima, H., Oka, K., Chan, L., and Maegawa, H. (2014). Gene therapy for neuropathic pain by silencing of TNF- α expression with lentiviral vectors targeting the dorsal root ganglion in mice. *PLoS ONE* 9, e92073.
7. Wagner, R., Janjigian, M., and Myers, R.R. (1998). Anti-inflammatory interleukin-10 therapy in CCI neuropathy decreases thermal hyperalgesia, macrophage recruitment, and endoneurial TNF-alpha expression. *Pain* 74, 35–42.
8. Zheng, C.X., Wang, S.M., Bai, Y.H., Luo, T.T., Wang, J.Q., Dai, C.Q., Guo, B.L., Luo, S.C., Wang, D.H., Yang, Y.L., and Wang, Y.Y. (2018). Lentiviral Vectors and Adeno-Associated Virus Vectors: Useful Tools for Gene Transfer in Pain Research. *Anat. Rec. (Hoboken)* 301, 825–836.
9. Glatzel, M., Flechsig, E., Navarro, B., Klein, M.A., Paterna, J.C., Büeler, H., and Aguzzi, A. (2000). Adenoviral and adeno-associated viral transfer of genes to the peripheral nervous system. *Proc. Natl. Acad. Sci. USA* 97, 442–447.
10. Xu, Y., Gu, Y., Xu, G.Y., Wu, P., Li, G.W., and Huang, L.Y. (2003). Adeno-associated viral transfer of opioid receptor gene to primary sensory neurons: a strategy to increase opioid antinociception. *Proc. Natl. Acad. Sci. USA* 100, 6204–6209.
11. Mason, M.R., Ehlert, E.M., Eggers, R., Pool, C.W., Hermening, S., Huseinovic, A., Timmermans, E., Blits, B., and Verhaagen, J. (2010). Comparison of AAV serotypes for gene delivery to dorsal root ganglion neurons. *Mol. Ther.* 18, 715–724.
12. Hammond, D.L., Ackerman, L., Holdsworth, R., and Elzey, B. (2004). Effects of spinal nerve ligation on immunohistochemically identified neurons in the L4 and L5 dorsal root ganglia of the rat. *J. Comp. Neurol.* 475, 575–589.
13. Fang, X., McMullan, S., Lawson, S.N., and Djouhri, L. (2005). Electrophysiological differences between nociceptive and non-nociceptive dorsal root ganglion neurones in the rat in vivo. *J. Physiol.* 565, 927–943.
14. Ruscheweyh, R., Forsthuber, L., Schoffnegger, D., and Sandkühler, J. (2007). Modification of classical neurochemical markers in identified primary afferent neurons with Abeta-, Adelta-, and C-fibers after chronic constriction injury in mice. *J. Comp. Neurol.* 502, 325–336.
15. Usoskin, D., Furlan, A., Islam, S., Abdo, H., Lönnerberg, P., Lou, D., Hjerling-Lefler, J., Haegström, J., Kharchenko, O., Kharchenko, P.V., et al. (2015). Unbiased classification of sensory neuron types by large-scale single-cell RNA sequencing. *Nat. Neurosci.* 18, 145–153.
16. Li, C.L., Li, K.C., Wu, D., Chen, Y., Luo, H., Zhao, J.R., Wang, S.S., Sun, M.M., Lu, Y.J., Zhong, Y.Q., et al. (2016). Somatosensory neuron types identified by high-coverage single-cell RNA-sequencing and functional heterogeneity. *Cell Res.* 26, 83–102.
17. Xie, R.G., Chu, W.G., Hu, S.J., and Luo, C. (2018). Characterization of Different Types of Excitability in Large Somatosensory Neurons and Its Plastic Changes in Pathological Pain States. *Int. J. Mol. Sci.* 19, 161.
18. Towne, C., Pertin, M., Beggah, A.T., Aebischer, P., and Decosterd, I. (2009). Recombinant adeno-associated virus serotype 6 (rAAV2/6)-mediated gene transfer to nociceptive neurons through different routes of delivery. *Mol. Pain* 5, 52.
19. Yu, H., Fischer, G., Ferhatovic, L., Fan, F., Light, A.R., Weihrauch, D., Sapunar, D., Nakai, H., Park, F., and Hogan, Q.H. (2013). Intraganglionic AAV6 results in efficient and long-term gene transfer to peripheral sensory nervous system in adult rats. *PLoS ONE* 8, e61266.
20. Iyer, S.M., Montgomery, K.L., Towne, C., Lee, S.Y., Ramakrishnan, C., Deisseroth, K., and Delp, S.L. (2014). Virally mediated optogenetic excitation and inhibition of pain in freely moving nontransgenic mice. *Nat. Biotechnol.* 32, 274–278.
21. Iyer, S.M., Vesuna, S., Ramakrishnan, C., Huynh, K., Young, S., Berndt, A., Lee, S.Y., Gorini, C.J., Deisseroth, K., and Delp, S.L. (2016). Optogenetic and chemogenetic strategies for sustained inhibition of pain. *Sci. Rep.* 6, 30570.
22. Jacques, S.J., Ahmed, Z., Forbes, A., Douglas, M.R., Vignesswara, V., Berry, M., and Logan, A. (2012). AAV8(gfp) preferentially targets large diameter dorsal root ganglion neurones after both intra-dorsal root ganglion and intrathecal injection. *Mol. Cell. Neurosci.* 49, 464–474.
23. Kubota, S., Sidikejiang, W., Kudo, M., Inoue, K.I., Umeda, T., Takada, M., and Seki, K. (2019). Optogenetic recruitment of spinal reflex pathways from large-diameter primary afferents in non-transgenic rats transduced with AAV9/Channelrhodopsin 2. *J. Physiol.* 597, 5025–5040.
24. Boada, D.M., Martin, T.J., Peters, C.M., Hayashida, K., Harris, M.H., Houle, T.T., Boyden, E.S., Eisenach, J.C., and Ririe, D.G. (2014). Fast-conducting mechanoreceptors contribute to withdrawal behavior in normal and nerve injured rats. *Pain* 155, 2646–2655.
25. Li, B., Yang, X.Y., Qian, F.P., Tang, M., Ma, C., and Chiang, L.Y. (2015). A novel analgesic approach to optogenetically and specifically inhibit pain transmission using TRPV1 promoter. *Brain Res.* 1609, 12–20.
26. Spencer, N.J., Hibberd, T.J., Lagerström, M., Otsuka, Y., and Kelley, N. (2018). Visceral pain - Novel approaches for optogenetic control of spinal afferents. *Brain Res.* 1693 (Pt B), 159–164.
27. Fischer, G., Pan, B., Vilceanu, D., Hogan, Q.H., and Yu, H. (2014). Sustained relief of neuropathic pain by AAV-targeted expression of CBD3 peptide in rat dorsal root ganglion. *Gene Ther.* 21, 44–51.
28. Watakabe, A., Ohtsuka, M., Kinoshita, M., Takaji, M., Isa, K., Mizukami, H., Ozawa, K., Isa, T., and Yamamori, T. (2015). Comparative analyses of adeno-associated viral vector serotypes 1, 2, 5, 8 and 9 in marmoset, mouse and macaque cerebral cortex. *Neurosci. Res.* 93, 144–157.
29. Gerits, A., Vancraeynest, P., Vreysen, S., Laramée, M.E., Michiels, A., Gijsbers, R., Van den Haute, C., Moons, L., Debyser, Z., Baekelandt, V., et al. (2015). Serotype-dependent transduction efficiencies of recombinant adeno-associated viral vectors in monkey neocortex. *Neurophotonics* 2, 031209.
30. Wu, S.H., Liao, Z.X., Rizak, J., Zheng, N., Zhang, L.H., Tang, H., He, X.B., Wu, Y., He, X.P., Yang, M.F., et al. (2017). Comparative study of the transfection efficiency of commonly used viral vectors in rhesus monkey (*Macaca mulatta*) brains. *Zool. Res.* 38, 88–95.
31. Watakabe, A., Sadakane, O., Hata, K., Ohtsuka, M., Takaji, M., and Yamamori, T. (2017). Application of viral vectors to the study of neural connectivities and neural circuits in the marmoset brain. *Dev. Neurobiol.* 77, 354–372.
32. Samaranch, L., Salegio, E.A., San Sebastian, W., Kells, A.P., Bringas, J.R., Forsayeth, J., and Bankiewicz, K.S. (2013). Strong cortical and spinal cord transduction after AAV7 and AAV9 delivery into the cerebrospinal fluid of nonhuman primates. *Hum. Gene Ther.* 24, 526–532.
33. Samaranch, L., Salegio, E.A., San Sebastian, W., Kells, A.P., Foust, K.D., Bringas, J.R., Lamarre, C., Forsayeth, J., Kaspar, B.K., and Bankiewicz, K.S. (2012). Adeno-associated virus serotype 9 transduction in the central nervous system of nonhuman primates. *Hum. Gene Ther.* 23, 382–389.
34. Gray, S.J., Nagabhushan Kalburgi, S., McCown, T.J., and Jude Samulski, R. (2013). Global CNS gene delivery and evasion of anti-AAV-neutralizing antibodies by intrathecal AAV administration in non-human primates. *Gene Ther.* 20, 450–459.
35. Matsuzaki, Y., Konno, A., Mochizuki, R., Shinohara, Y., Nitta, K., Okada, Y., and Hirai, H. (2018). Intravenous administration of the adeno-associated virus-PHP.B capsid fails to upregulate transduction efficiency in the marmoset brain. *Neurosci. Lett.* 665, 182–188.
36. Rigaud, M., Gemes, G., Barabas, M.E., Chernoff, D.I., Abram, S.E., Stucky, C.L., and Hogan, Q.H. (2008). Species and strain differences in rodent sciatic nerve anatomy: implications for studies of neuropathic pain. *Pain* 136, 188–201.
37. Ma, Q.P. (2002). Expression of capsaicin receptor (VR1) by myelinated primary afferent neurons in rats. *Neurosci. Lett.* 319, 87–90.
38. Amaya, F., Decosterd, I., Samad, T.A., Plumpton, C., Tate, S., Mannion, R.J., Costigan, M., and Woolf, C.J. (2000). Diversity of expression of the sensory neuron-specific TTX-resistant voltage-gated sodium ion channels SNS and SNS2. *Mol. Cell. Neurosci.* 15, 331–342.
39. Hilliard, K.A., Blahó, V.A., Jackson, C.D., and Brown, C.R. (2020). Leukotriene B4 receptor BLT1 signaling is critical for neutrophil apoptosis and resolution of experimental Lyme arthritis. *FASEB J.* 34, 2840–2852.
40. Hordeaux, J., Buza, E.L., Dyer, C., Goode, T., Mitchell, T.W., Richman, L., Denton, N., Hinderer, C., Katz, N., Schmid, R., et al. (2020). Adeno-Associated Virus-Induced Dorsal Root Ganglion Pathology. *Hum. Gene Ther.* 31, 808–818.
41. Lu, C.R., Hwang, S.J., Phend, K.D., Rustioni, A., and Valtchanoff, J.G. (2002). Primary afferent terminals in spinal cord express presynaptic AMPA receptors. *J. Neurosci.* 22, 9522–9529.
42. Todd, A.J., Hughes, D.I., Polgár, E., Nagy, G.G., Mackie, M., Ottersen, O.P., and Maxwell, D.J. (2003). The expression of vesicular glutamate transporters VGLUT1

- and VGLUT2 in neurochemically defined axonal populations in the rat spinal cord with emphasis on the dorsal horn. *Eur. J. Neurosci.* *17*, 13–27.
43. Towne, C., Schneider, B.L., Kieran, D., Redmond, D.E., Jr., and Aebischer, P. (2010). Efficient recombination of non-human primate motor neurons after intramuscular delivery of recombinant AAV serotype 6. *Gene Ther.* *17*, 141–146.
 44. Towne, C., Montgomery, K.L., Iyer, S.M., Deisseroth, K., and Delp, S.L. (2013). Optogenetic control of targeted peripheral axons in freely moving animals. *PLoS ONE* *8*, e72691.
 45. Foust, K.D., Nurre, E., Montgomery, C.L., Hernandez, A., Chan, C.M., and Kaspar, B.K. (2009). Intravascular AAV9 preferentially targets neonatal neurons and adult astrocytes. *Nat. Biotechnol.* *27*, 59–65.
 46. Pexton, T., Moeller-Bertram, T., Schilling, J.M., and Wallace, M.S. (2011). Targeting voltage-gated calcium channels for the treatment of neuropathic pain: a review of drug development. *Expert Opin. Investig. Drugs* *20*, 1277–1284.
 47. Piekarczyk, A.D., Due, M.R., Khanna, M., Wang, B., Ripsch, M.S., Wang, R., Meroueh, S.O., Vasko, M.R., White, F.A., and Khanna, R. (2012). CRMP-2 peptide mediated decrease of high and low voltage-activated calcium channels, attenuation of nociceptor excitability, and anti-nociception in a model of AIDS therapy-induced peripheral neuropathy. *Mol. Pain* *8*, 54.
 48. Yu, H., Shin, S.M., Xiang, H., Chao, D., Cai, Y., Xu, H., Khanna, R., Pan, B., and Hogan, Q.H. (2019). AAV-encoded Ca_v2.2 peptide aptamer CBD3A6K for primary sensory neuron-targeted treatment of established neuropathic pain. *Gene Ther.* *26*, 308–323.
 49. Xiang, H., Liu, Z., Wang, F., Xu, H., Roberts, C., Fischer, G., Stucky, C., Caron, D., Pan, B., Hogan, Q., and Yu, H. (2017). Primary sensory neuron-specific interference of TRPV1 signaling by AAV-encoded TRPV1 peptide aptamer attenuates neuropathic pain. *Mol. Pain* *13*, 1744806917717040.
 50. Fischer, K.B., Collins, H.K., and Callaway, E.M. (2019). Sources of off-target expression from recombinase-dependent AAV vectors and mitigation with cross-over insensitive ATG-out vectors. *Proc. Natl. Acad. Sci. USA* *116*, 27001–27010.
 51. Vulchanova, L., Schuster, D.J., Belur, L.R., Riedl, M.S., Podetz-Pedersen, K.M., Kitto, K.F., Wilcox, G.L., McIvor, R.S., and Fairbanks, C.A. (2010). Differential adeno-associated virus mediated gene transfer to sensory neurons following intrathecal delivery by direct lumbar puncture. *Mol. Pain* *6*, 31.
 52. Schuster, D.J., Dykstra, J.A., Riedl, M.S., Kitto, K.F., Belur, L.R., McIvor, R.S., Elde, R.P., Fairbanks, C.A., and Vulchanova, L. (2014). Biodistribution of adeno-associated virus serotype 9 (AAV9) vector after intrathecal and intravenous delivery in mouse. *Front. Neuroanat.* *8*, 42.
 53. Puljak, L., Kojundzic, S.L., Hogan, Q.H., and Sapunar, D. (2009). Targeted delivery of pharmacological agents into rat dorsal root ganglion. *J. Neurosci. Methods* *177*, 397–402.
 54. Fischer, G., Kostic, S., Nakai, H., Park, F., Sapunar, D., Yu, H., and Hogan, Q. (2011). Direct injection into the dorsal root ganglion: technical, behavioral, and histological observations. *J. Neurosci. Methods* *199*, 43–55.
 55. Deverman, B.E., Pravdo, P.L., Simpson, B.P., Kumar, S.R., Chan, K.Y., Banerjee, A., Wu, W.L., Yang, B., Huber, N., Pasca, S.P., and Gradinaru, V. (2016). Cre-dependent selection yields AAV variants for widespread gene transfer to the adult brain. *Nat. Biotechnol.* *34*, 204–209.
 56. Chan, K.Y., Jang, M.J., Yoo, B.B., Greenbaum, A., Ravi, N., Wu, W.L., Sánchez-Guardado, L., Lois, C., Mazmanian, S.K., Deverman, B.E., and Gradinaru, V. (2017). Engineered AAVs for efficient noninvasive gene delivery to the central and peripheral nervous systems. *Nat. Neurosci.* *20*, 1172–1179.
 57. Zhou, L., Népote, V., Rowley, D.L., Levacher, B., Zvara, A., Santha, M., Mi, Q.S., Simonneau, M., and Donovan, D.M. (2002). Murine peripherin gene sequences direct Cre recombinase expression to peripheral neurons in transgenic mice. *FEBS Lett.* *523*, 68–72.
 58. Nitta, K., Matsuzaki, Y., Konno, A., and Hirai, H. (2017). Minimal Purkinje Cell-Specific PCP2/L7 Promoter Virally Available for Rodents and Non-human Primates. *Mol. Ther. Methods Clin. Dev.* *6*, 159–170.
 59. Matsuzaki, Y., Konno, A., Mukai, R., Honda, F., Hirato, M., Yoshimoto, Y., and Hirai, H. (2017). Transduction Profile of the Marmoset Central Nervous System Using Adeno-Associated Virus Serotype 9 Vectors. *Mol. Neurobiol.* *54*, 1745–1758.
 60. Hinderer, C., Katz, N., Buza, E.L., Dyer, C., Goode, T., Bell, P., Richman, L.K., and Wilson, J.M. (2018). Severe Toxicity in Nonhuman Primates and Piglets Following High-Dose Intravenous Administration of an Adeno-Associated Virus Vector Expressing Human SMN. *Hum. Gene Ther.* *29*, 285–298.
 61. Hordeaux, J., Hinderer, C., Goode, T., Buza, E.L., Bell, P., Calcedo, R., Richman, L.K., and Wilson, J.M. (2018). Toxicology Study of Intra-Cisterna Magna Adeno-Associated Virus 9 Expressing Iduronate-2-Sulfatase in Rhesus Macaques. *Mol. Ther. Methods Clin. Dev.* *10*, 68–78.
 62. Hordeaux, J., Hinderer, C., Goode, T., Katz, N., Buza, E.L., Bell, P., Calcedo, R., Richman, L.K., and Wilson, J.M. (2018). Toxicology Study of Intra-Cisterna Magna Adeno-Associated Virus 9 Expressing Human Alpha-L-Iduronidase in Rhesus Macaques. *Mol. Ther. Methods Clin. Dev.* *10*, 79–88.
 63. Orsi, A., Rees, D., Andreini, I., Venturella, S., Cinelli, S., and Oberto, G. (2011). Overview of the marmoset as a model in nonclinical development of pharmaceutical products. *Regul. Toxicol. Pharmacol.* *59*, 19–27.
 64. Mattar, C.N., Waddington, S.N., Biswas, A., Johana, N., Ng, X.W., Fisk, A.S., Fisk, N.M., Tan, L.G., Rahim, A.A., Buckley, S.M., et al. (2013). Systemic delivery of scAAV9 in fetal macaques facilitates neuronal transduction of the central and peripheral nervous systems. *Gene Ther.* *20*, 69–83.
 65. Bevan, A.K., Duque, S., Foust, K.D., Morales, P.R., Braun, L., Schmelzer, L., Chan, C.M., McCrate, M., Chicoine, L.G., Coley, B.D., et al. (2011). Systemic gene delivery in large species for targeting spinal cord, brain, and peripheral tissues for pediatric disorders. *Mol. Ther.* *19*, 1971–1980.
 66. Gray, S.J., Matagne, V., Bachaboina, L., Yadav, S., Ojeda, S.R., and Samulski, R.J. (2011). Preclinical differences of intravascular AAV9 delivery to neurons and glia: a comparative study of adult mice and nonhuman primates. *Mol. Ther.* *19*, 1058–1069.
 67. Brooks, A.R., Harkins, R.N., Wang, P., Qian, H.S., Liu, P., and Rubanyi, G.M. (2004). Transcriptional silencing is associated with extensive methylation of the CMV promoter following adenoviral gene delivery to muscle. *J. Gene Med.* *6*, 395–404.
 68. Yang, Y., Mariati, Chusainow, J., and Yap, M.G. (2010). DNA methylation contributes to loss in productivity of monoclonal antibody-producing CHO cell lines. *J. Biotechnol.* *147*, 180–185.
 69. Kato, S., Kuramochi, M., Takasumi, K., Kobayashi, K., Inoue, K., Takahara, D., Hitoshi, S., Ikenaka, K., Shimada, T., Takada, M., and Kobayashi, K. (2011). Neuron-specific gene transfer through retrograde transport of lentiviral vector pseudotyped with a novel type of fusion envelope glycoprotein. *Hum. Gene Ther.* *22*, 1511–1523.
 70. Gusel'nikova, V.V., and Korzhevskiy, D.E. (2015). NeuN As a Neuronal Nuclear Antigen and Neuron Differentiation Marker. *Acta Naturae* *7*, 42–47.